REPORT DOCUMENTATION PAGE

Public reporting burden for this collection of information is estimated to average 1 hour per response, including the time for reviewing instructions, searching existing data sources, gathering and maintaining the data needed, and completing and reviewing the collection of information. Send comment regarding this burden estimates or any other aspect of this collection of information, including suggestions for reducing this burden, to Washington Headquarters Services, Directorate for information Operations and Reports, 1215 Jefferson Davis Highway, Suite 1204, Arlington, VA 22202-4302, and to the Office of Management and Budget, Paperwork Reduction Project (0704-0188), Washington, DC 20503.

1. AGENCY USE ONLY *(Leave blank)*	2. REPORT DATE 29 September 97	3. REPORT TYPE AND DATES COVERED FINAL REPORT 14 April 94 – 6 June 97

4. TITLE AND SUBTITLE

Near-field Scanning Optical Microscopy and Spectroscopy

5. FUNDING NUMBERS

DAAH04-94-G-0064

6. AUTHOR(S)

M. A. Paesler and B. I. Yakobson

7. PERFORMING ORGANIZATION NAMES(S) AND ADDRESS(ES)

Physics Department
N.C. State University
Box 8202
Raleigh, NC 27695-8202

8. PERFORMING ORGANIZATION REPORT NUMBER

9. SPONSORING / MONITORING AGENCY NAME(S) AND ADDRESS(ES)

U.S. Army Research Office
P.O. Box 12211
Research Triangle Park,, NC 27709-2211

10. SPONSORING / MONITORING AGENCY REPORT NUMBER

32434.1-PH

11. SUPPLEMENTARY NOTES

The views, opinions and/or findings contained in this report are those of the author(s) and should not be construed as an official Department of the Army position, policy or decision, unless so designated by other documentation.

12a. DISTRIBUTION / AVAILABILITY STATEMENT

Approved for public release; distribution unlimited.

19971204 113

13. ABSTRACT *(Maximum 200 words)*

The near-field scanning optical microscope, or NSOM, provides spatial resolution of surface features considerably smaller than the wavelength of the radiation used to image. We have focused on both the development and the use of the NSOM. In the former, we considered the confinement of optical fields to nanometric structures. We analyzed the delivery of light from the far-field to the near-field region in tapered optical fibers. Our analysis led to the design and development of near-field probes of that allow for the performance of relatively light-starved NSOM experiments. Using such probes, we have demonstrated a capability of using spectral contrast in near-field imaging. In studies of KTP, for example, we have performed nano-Raman spectroscopy samples, and have imaged sub-wavelength surfaces features using only Raman-scattered light. In ongoing research we have launced further efforts to improve probe design and have begun nano-Raman investigations Mercry Cadmium Telluride and semiconducting diamond.

14. SUBJECT TERMS

Near-field Optics

DTIC QUALITY INSPECTED 4

15. NUMBER IF PAGES

22

16. PRICE CODE

17. SECURITY CLASSIFICATION OR REPORT	18. SECURITY CLASSIFICATION OF THIS PAGE	19. SECURITY CLASSIFICATION OF ABSTRACT	20. LIMITATION OF ABSTRACT
UNCLASSIFIED	UNCLASSIFIED	UNCLASSIFIED	UL

GENERAL INSTRUCTIONS FOR COMPLETING SF 298

The Report Documentation Page (RDP) is used in announcing and cataloging reports. It is important that this information be consistent with the rest of the report, particularly the cover and title page. Instructions for filling in each block of the form follow. It is important to *stay within the lines* to meet *optical scanning requirements.*

Block 1. Agency Use Only *(Leave blank)*

Block 2. Report Date. Full publication date including day, month, and year, if available (e.g. 1 Jan 88). Must cite at least year.

Block 3. Type of Report and Dates Covered. State whether report is interim, final, etc. If applicable, enter inclusive report dates (e.g. 10 Jun 87 - 30 Jun 88).

Block 4. Title and Subtitle. A title is taken from the part of the report that provides the most meaningful and complete information. When a report is prepared in more than one volume, repeat the primary title, add volume number, and include subtitle for the specific volume. On classified documents enter the title classification in parentheses.

Block 5. Funding Numbers. To include contract and grant numbers; may include program element number(s), project number(s), task number(s), and work unit number(s). Use the following labels:

```
C  - Contract      PR - Project
G  - Grant         TA - Task
PE - Program       WU - Work Unit
     Element            Accession No.
```

Block 6. Author(s). Name(s) of person(s) responsible for writing the report, performing the research, or credited with the content of the report. If editor or compiler, this should follow the name(s).

Block 7. Performing Organization Name(s) and Address(es). Self-explanatory.

Block 8. Performing Organization Report Number. Enter the unique alphanumeric report number(s) assigned by the organization performing the report.

Block 9. Sponsoring/Monitoring Agency Name(s) and Address(es). Self-explanatory.

Block 10. Sponsoring/Monitoring Agency Report Number. *(If known)*

Block 11. Supplementary Notes. Enter information not included elsewhere such as; prepared in cooperation with...; Trans. of...; To be published in.... When a report is revised, include a statement whether the new report supersedes or supplements the older report.

Block 12a. Distribution/Availability Statement. Denotes public availability or limitations. Cite any availability to the public. Enter additional limitations or special markings in all capitals (e.g. NORFORN, REL, ITAR).

```
DOD  - See DoDD 4230.25, "Distribution
         Statements on Technical
         Documents."
DOE  - See authorities.
NASA - See Handbook NHB 2200.2.
NTIS - Leave blank.
```

Block 12b. Distribution Code.

```
DOD  - Leave blank
DOE  - Enter DOE distribution categories
         from the Standard Distribution for
         Unclassified Scientific and Technical
         Reports
NASA - Leave blank.
NTIS - Leave blank.
```

Block 13. Abstract. Include a brief *(Maximum 200 words)* factual summary of the most significant information contained in the report.

Block 14. Subject Terms. Keywords or phrases identifying major subjects in the report.

Block 15. Number of Pages. Enter the total number of pages.

Block 16. Price Code. Enter appropriate price code *(NTIS only)*.

Block 17. - 19. Security Classifications. Self-explanatory. Enter U.S. Security Classification in accordance with U.S. Security Regulations (i.e., UNCLASSIFIED). If form contains classified information, stamp classification on the top and bottom of the page.

Block 20. Limitation of Abstract. This block must be completed to assign a limitation to the abstract. Enter either UL (unlimited) or SAR (same as report). An entry in this block is necessary if the abstract is to be limited. If blank, the abstract is assumed to be unlimited.

Near-field Scanning Optical Microscopy and Spectrsocopy

FINAL PROGRESS REPORT

Michael Paesler
Boris Yakobson

29 September 1997

U.S. ARMY RESEARCH OFFICE

DAAH04-94-G-0064

Physics Department
North Carolina State University
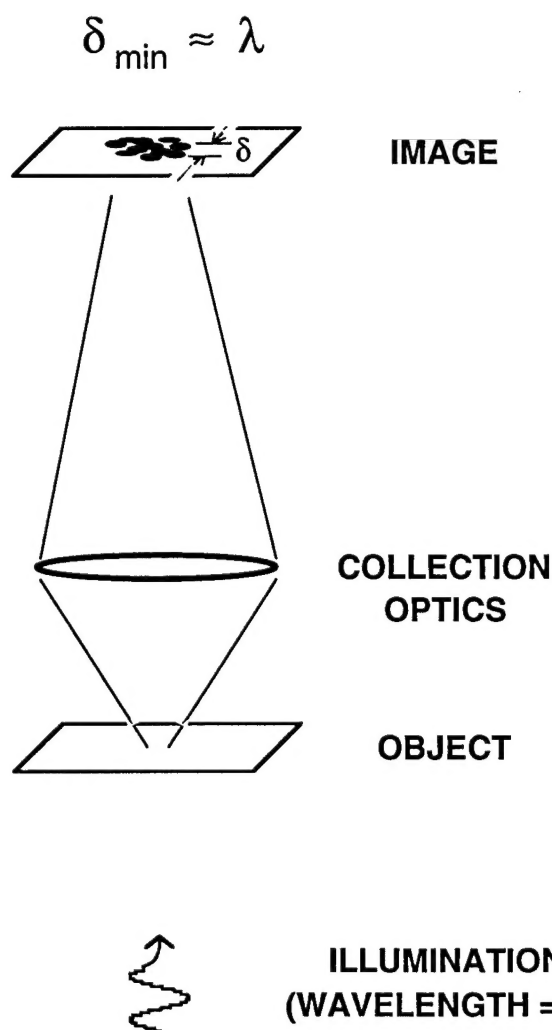Raleigh, NC 27695-8202

APPROVED FOR PUBLIC RELEASE

DISTRIBUTION UNLIMITED

1. FOREWARD

The near-field scanning optical microscope, or NSOM, has established itself as the champion of spatial resolution[1, 2] in the arena of optical investigations. The finer spatial resolution - made possible with the use of a sharpened fiber - is shown schematically in Figure 1.

CONVENTIONAL OPTICAL MICROSCOPE

NEAR FIELD SCANNING OPTICAL MICROSCOPE, NSOM

$$\delta_{min} \approx \lambda$$

$$\delta_{min} \ll \lambda$$

IMAGE

COLLECTION OPTICS

OBJECT

detector

x

scan

y

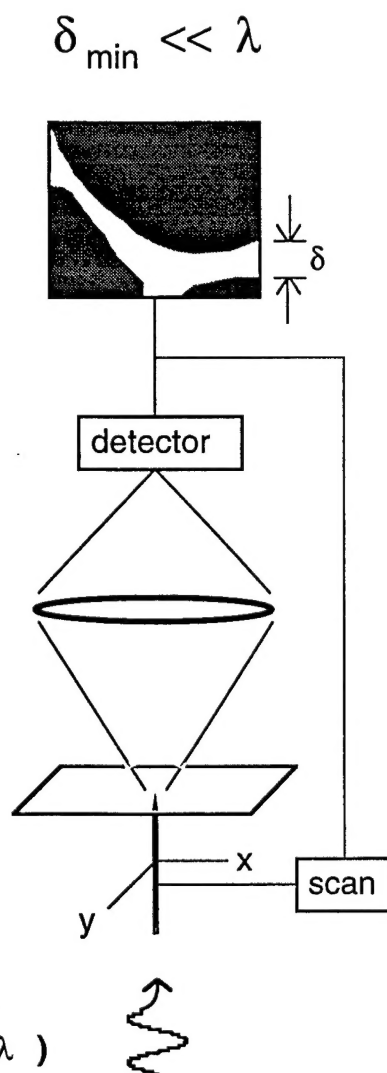ILLUMINATION (WAVELENGTH = λ)

Figure 1.

Comparison of conventional optical micrsocope and an NSOM. Both instruments presume illumination from below.

The illustration compares a conventional optical microscope and an NSOM. For clarity, both instruments are presumed to be configured with an object illuminated with light of wavelength λ from below. The conventional image is collected in a parallel manner and lateral spatial resolution δ_{min} (which is far-field difraction limited) is on the order of the wavelength of the probe radiation λ. In this illumination mode NSOM, the sharpened taper is scanned in the x-y plane, and the signal measured in the detector is correlated with the position of the taper to reconstruct the image that can have resolution $\delta_{min} < \lambda$ as shown.

Our research program has focused on two specific number of fronts: i) to develop the NSOM's capabilities, and ii) to use the NSOM's proven capabilities in novel research. Thus, this report highlights our results in both instrument *development* and instrument *use*.

2. TABLE OF CONTENTS

3. STATMENT OF THE PROBLEM STUDIED

The confinement of optical fields to sub-wavelength dimensions in the near-field scanning optical microscope, or NSOM, manifests itself in investigations in materials science, surface chemistry, molecular biology, and other disciplines. The family of NSOM problems we studied in the course of the ARO-funded research centered on developing the capabilities of the NSOM and in using them in a number of interesting materials studies.

In many applications, the most severe limitation on system performance is signal intensity. Our efforts in instrument development centered largely on analyzing the light-delivery in an NSOM with a goal of increasing the flux delivered to the near-field region. We were successful in enhancing the light flux passed through this through careful analysis of system design. Our studies also led to suggestions for the next generation of near-field probes that provides one of the bases for futhre work.

Our materials-centered investigations revolved around two specific problems: the feasibility of doing nano-Raman spectrsocopy with the NSOM, and the use of time as a contrast mechanism in NSOM research. For the former, we provided the first nano-Raman NSOM images using samples of KTP. For the latter, our studies of carrier dynamics in Si provided the first example of time-resolved sample contrast in near-field imaging.

4. SUMMARY OF IMPORTANT RESULTS

Our research in near-field optics has progressed along a number of fronts. In the following we first briefly review the highlights of our research program (section A). This review emphasizes in particular the developments that we initiated in near-field research. Following this, we discuss in more detail three specific advances (sections B, C, and D) that will provide springboards for future research.

A. Research Highlights.

• We were the first laboratory to perform spectroscopic near-field measurements. Our studies of stressed sapphire showed that one could map stress profiles using a near-field microscope[3, 4].

• Ours was the first to perform cryogenic near-field imaging. Our images of the surface of sapphire demonstrated that a near-field instrument could be made to work at cryogenic temperatures[5].

• We were the first to develop a shear-force near-field microscope that operated in the reflection mode[6].

- We proposed first theoretical model of the probe-forming process[7, 8] which became a reference for further studies by many groups[9, 10], and a guide for technological improvements.

- Ours was the first laboratory to employ vertical dithering as a means of image enhancement in near-field imaging[11, 12].

- We were among the first laboratories to demonstrate that polarization contrast could be employed in near-field imaging[12].

- We were the first to show how time could be used as a contrast mechanism in near-field imaging[13].

- We were among the first to measure the elevated operating temperature of the NSOM taper[14].

- We were the first to model NSOM taper optics[15] and to explain the inefficiency involved with delivery of light from the far- to the near-field regions[16].

- We were the first to demonstrate the possibility of using varying penetration depths to enable depth profiling of subsurface stress in microRaman studies[17, 18].

- We were the first laboratory to perform Raman near-field imaging[19].

B. Nano-Raman Spectroscopy with the NSOM.

Raman spectroscopy is a powerful analytical tool that can be used to determine - for example - sample chemistry, stress state, amorphicity or composition. We used our reflection-collection mode NSOM with shear force distance control to investigate KTP (potassium titanyl phosphate), which is a non-linear optical material used for surface second harmonic generation applications. Images are shown in figure 2.

Figures 2a and 2b are the shear force and optical images of a 10 μm x 10 μm region of the sample. The square region in each image identifies the Rb-doped section of the sample. The relatively large Rb atom causes the matrix to expand. This manifests itself in a terrace approximately 2nm above the plane of the undoped sample as can be seen in the topographic image. Optical contrast in figure 2b tracks the topographic image closely. Figure 2c is a 4 μm x 4 μm region near the corner of the doped region. Again the topographic image indicates the expanded matrix in the doped region.

60 nm

0 nm

1μm

Intensity
8.7 nm   10 (arbitrary units)
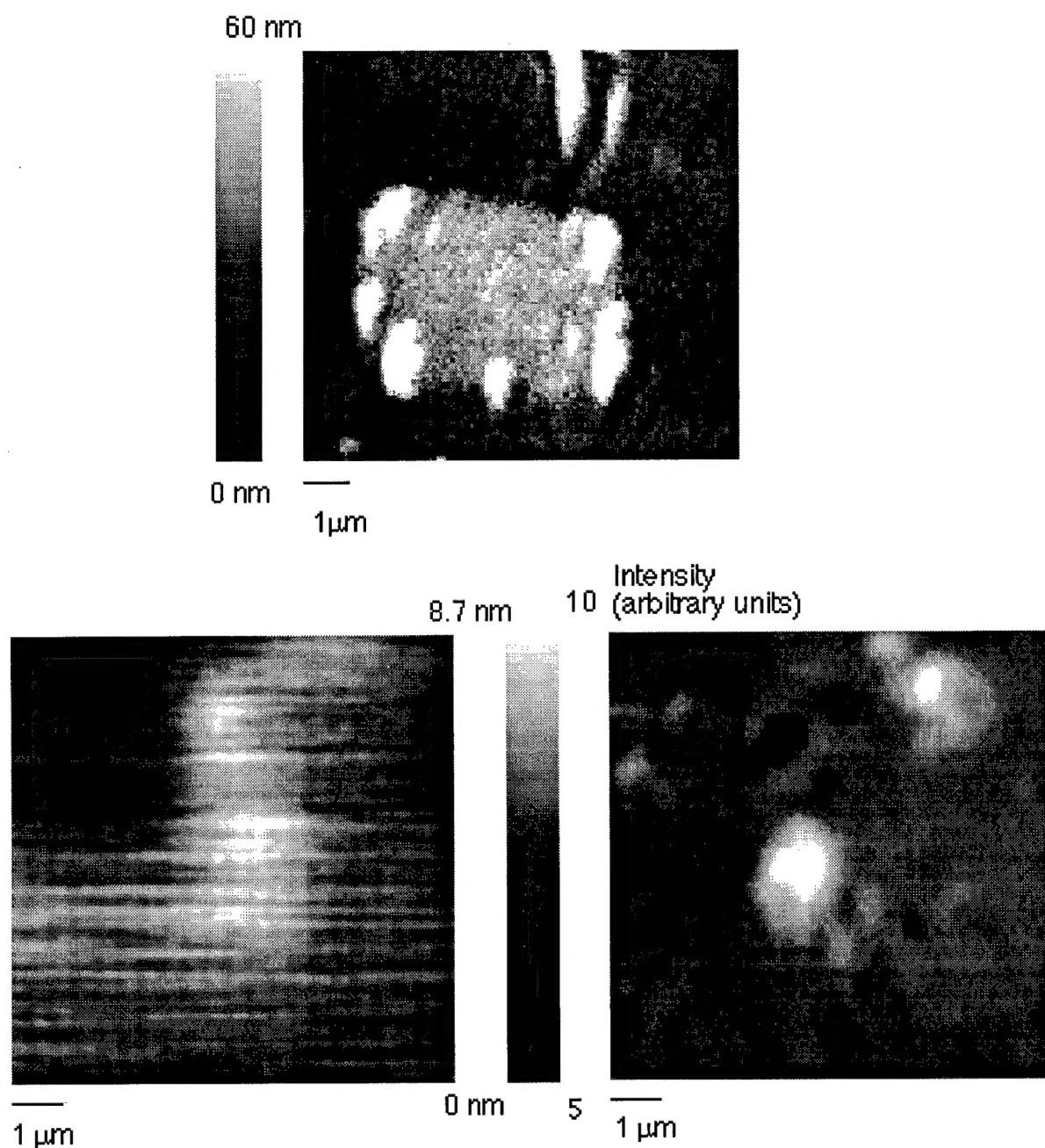
0 nm   5

1 μm

1 μm

Figure 2.
a) A 10 μm square shear-force image of the KTP surface. The light spot is the Rb-doped region. b) An NSOM image of the same region. c) An NSOM image of a 2 μm square region of the lower right corner of the doped region of the same surface. d) An NSOM image of the same region taken with Raman scattered light at 767 cm^{-1}.

5

Raman spectra above doped and undoped regions of the sample are shown in figure 3. The strong feature at 767 cm^{-1} is an A1 vibrational mode assigned to the TiO$_6$ stretching mode. Its relative strength is considerably greater in the Rb-doped region of the sample. By tuning the spectrometer to this feature and taking an image in the Raman scattered light, one obtains the image shown in figure 2d. The source of the contrast in this image is the slight index difference between the Rb-doped and the undoped regions.

Figure 3.

Near-field Raman spectra taken in two regions of the sample imaged in figure 2. The upper trace was taken over the Rb-doped region. The lower trace was taken over the un-doped region.
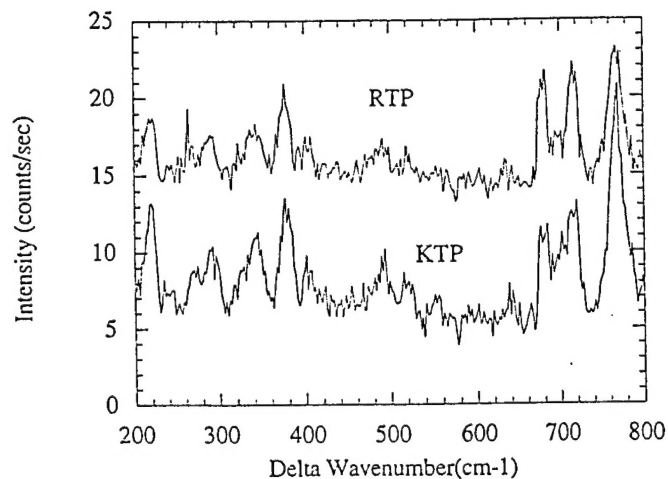
These nano-Raman results represent significant advances in near-field imaging. The low quantum efficiency of the Raman effect and the low throughput of the NSOM tip led many to believe that imaging *within* a Raman line could not be done. These data show that such imaging is indeed possible. To obtain images, a very stable microscope had to be built. The microscope used has a drift rate of 3Å/min corresponding to a 200 nm drift over the duration of the imaging scan. Drift currently limits the resolution.

This example of spectral imaging demonstrates that near-field microscopy can be undertaken when the source of the contrast is something as subtle as the slight index difference between doped and un-doped regions of a sample. On the other hand, it underscores the need for continued probe improvement. Enhancement probe efficiency would enable us to study even weaker effects with current scan rates and times. Perhaps more importantly, it would enable us to obtain spectroscopic images in much shorter times.

C. Modeling Taper Optics. Our systematic studies of the probe began with the nanomechanics of the taper making[7, 8]. This work logically led us to consider the optics of tapered fibers. While the literature about lenses is voluminous, the optics of the aluminum coated NSOM taper is scarcely discussed. It is experimentally observed, however, that optical signals weaken

dramatically on the way through the tapered fiber. Our studies have shown that:

- for milliwatts of input power, the taper delivers nanowatts through the near-field region;
- increased input power results in damage to the aluminum coating and thus destruction of the taper as a near-field probe;
- the damage threshold is set by the sideput density (the power per unit area absorbed by the aluminum coating) at a distance of tens to hundreds of microns from the taper apex.

We have modeled optical transmission in NSOM probes and have determined that the sideput density - and thus the damage threshold - is strongly dependent upon taper shape. In figure 4 we show the sideput density as a function of distance from the taper for a variety of taper shapes. The curves range from a linear taper (LP=1) to a parabolic taper (LP=0). The parabolic taper results in a demonstrably diminshed sideput density. With this optical modeling of the taper, we have set out to obtain a quantitative insight and to develop an intuition which will be useful in suggesting improvements in taper performance and manufacture.
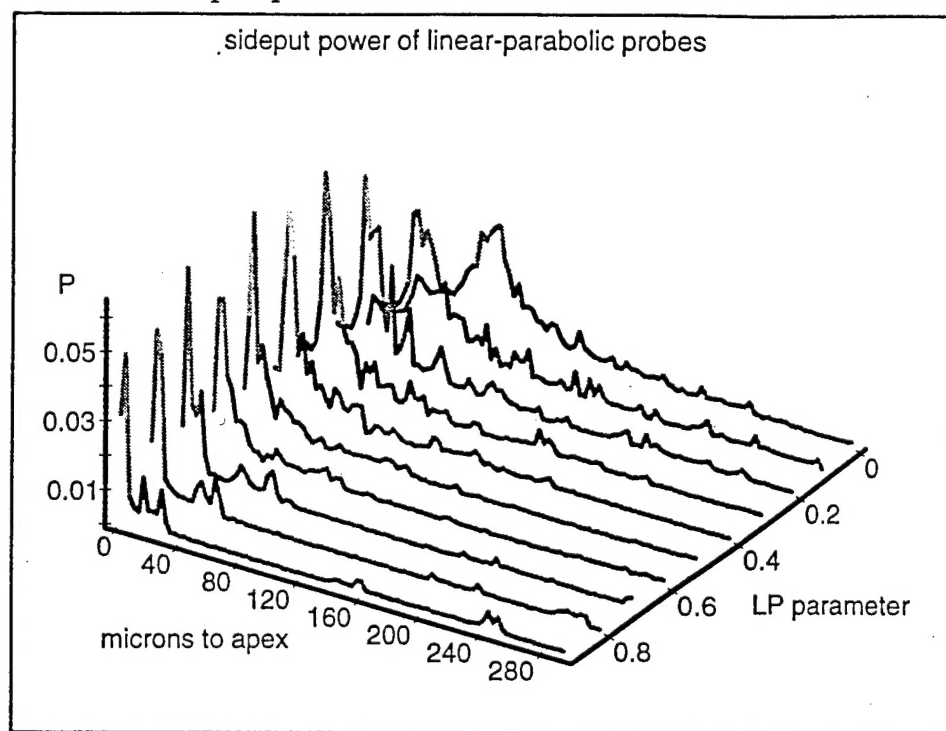

Figure 4.
Calculated energy sideput distribution as a function of distance from the taper apex for several taper shapes. Each of the 10 curves represents a different shape from a linear cone (LP=1) to a paraboloid of revolution (LP=0). For all shapes, the large majority of the sideput is distributed several microns from the taper apex.

7

D. Mapping Carrier Dynamics. Time resolved imaging is an active area of research in both conventional[20] and near-field[21, 22] optics. One can use the dynamics of physical processes to image specific materials features. In our semiconductor studies, for example, we investigate local variation in the relaxation of photo-excited carriers generated by optical pulses. The carriers are detected by monitoring their effect on the optical absorption at much longer wavelengths.

In operation, we obtain topographic (shear-force) NSOM images of semiconductor surfaces while we simultaneously measure IR transmission. By adding pulsed visible radiation to the NSOM illumination, we create a modulated population of photo-excited carriers. Then by detecting the change in IR absorption at the frequency of the pulsed visible radiation, we are able to image carrier lifetimes with the NSOM. Since lifetimes are very dependent on defects and impurities, the image taken in this manner becomes an image of defect populations.

E. Ongoing Research Objectives

Near-field optics advances along two distinct fronts. On one hand, the discipline is young and the technologies are immature. Thus important progress can still be made in fundamental understanding of near-field interactions and the design of near-field instruments. On the other hand, the technologies are in some senses well-developed. Thus subwavelength microscopies, spectroscopies, and materials processing applications are currently at hand. We have contiuned to focus our program on both of these fronts. In the following we review progress and outline a program of our future efforts.

1. Near-field Research

Near-field insturments are phenomenally inefficient. Whether one considers imaging with the near-field scanning optical microscope (NSOM) or signal processing with a near-field probe, the injection of milliwatts of power into a near-field device generally results in the couping of nanowatts of power into the near-field region of interest. The imaging applications proposed below are plagued by low intensities. Improvements of light coupling in near-field devices will lead to enhanced applications capabilities even beyond thos proposed here.

The throughput T of a near-field device is a product of three factors. That is,

$$T = (1 - L_{nf}) \times (1 - L_{ff}) \times \Theta \left(\frac{\text{input power}}{\text{breakdown threshold}} \right) \qquad (1)$$

8

Here the normalized near- and far-field losses are L_{nf} and L_{ff} respectively, and a step function Θ refelects the breakdown threshold. Θ is either 1 or 0 depending on whether its argument is less than or greater than one.

We have argued[16] that in illumination applications, the limit to increased coupled light lies in the relatively low breakdown threshold of an NSOM taper. This in turn is a function of what is called the sideput density.

For metal-coated tapered optical fibers in common use, the breakdown threshold is determined by the sideput density tens to hundreds of microns from the apex of the tip as seen in figure 4. Calculations suggest that the aperture could withstand and transmit intensties one or two orders of magnitude higher than those currently delivered at the breakdown threshold. Thus, ten- or even hundred-fold improvements in T could be obtained if the sideput density in the far-field region could be decreased. We propose to develop new taper designs that should lead to such an improvement.

a. Metal Annulus Probe. One result of our studies of taper optics suggests that *a metallic coating is not needed along most of the NSOM taper.* This can be seen in figure 5, where we show the angle the incident light makes with the normal along the taper. Each point on this plot represents an interaction of light with the glass-metal interface. The points merge into curves that represent a bundle interacting with the interface.
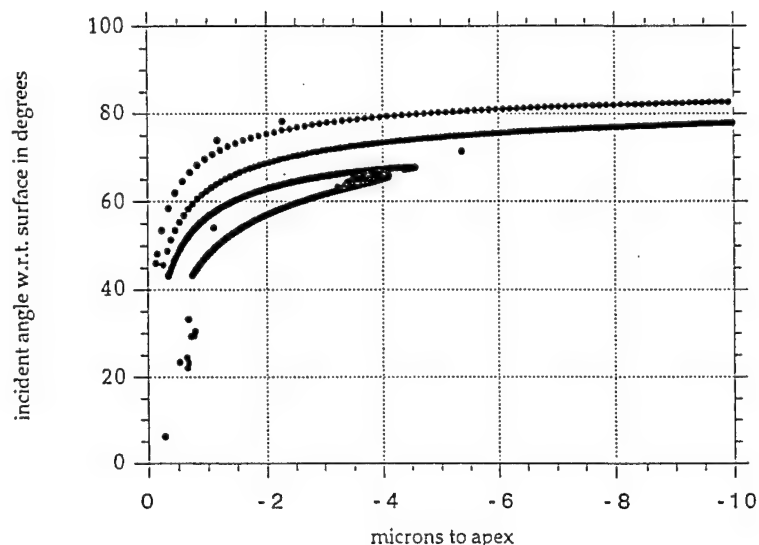

Figure 5.
The incident angle of light on the taper wall as a function of distance to the apex for one particular probe. Each point on any of the curves represents an interaction of light with the cladding-air interface. For the cladding used, the critical angle is 43°. (Note that angles are measured with respect to the fiber axis.)

9

One can read figure 5 along the taper from the fiber to the apex (i.e. from right to left). First, light in the core is ejected to the cladding. Next, an interaction with the metal coating occurs. As the apex is approached the incident angle decreases as more and more encounters take place. Only very close to the apex is the incident angle less than 43°the critical angle for total internal reflection for light incident upon a cladding/air interface. (We assume n = 1.46 for the fiber cladding.)

The information of Figure 5 is particularly intriguing given the sideput density profile for the same taper. This is shown in figure 6. Here we see that a large fraction of the sideput occurs at distances from the apex > 10 μm. Thus, if the taper were not coated, there would be no sideput density problem - and thus no breakdown problem - caused by light interacting with the metal along the taper.
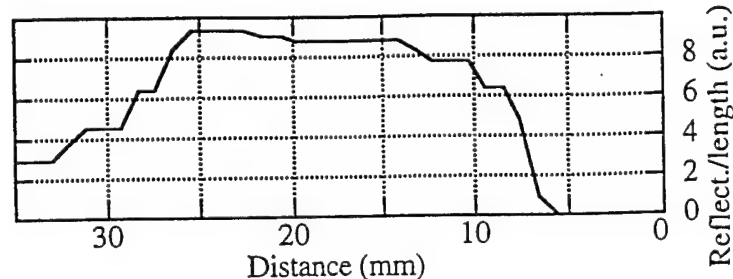

Figure 6.
The sideput density as a function of distance from the apex for the taper modelled in figure 5. The great majority of sideput is distributed at distances greater than about 10 μm from the apex.

Of course the optical field cannot be confined to sub-wavelength dimensions by a dielectric tip[11, 23] so a metal aperture is needed. But the data of figures 5 and 6 suggest that this aperture might best be made to extend only about 10 μm from the apex. We propose to construct such a taper and to explore its use. We expect that its breakdown threshold will be significantly higher than a fully-coated similar tip. We expect that the apex itself may be able to withstand significantly larger intenstities than those currently delivered to it by a fully-coated taper.

Our attempts to create such a taper will involve etching techniques. We will coat the entire taper, leaving a subwavelength aperture at the apex. Then we will encapsulate a small region from the apex up the shaft for a distance of approximately 10 μm. We will then etching away the Al and finally remove the encapsulant to reveal the required metallic annulus.

10

b. Taper Manufacture. The large majority of NSOM tips in current use are made by coating tapers made in pipette pullers[1, 7, 24]. While such manufacture has proven successful, it must be admitted that the process is difficult to control and generally not reproducible. Only because one can pull a large of number of tips with little difficulty has it become possible to produce the occasional good tip needed for an NSOM.

Experience shows that a positive curvature along the taper and an apex angle of roughly 45° seems to provide a high-throughput, high damage threshold tip. Optical modelling results have also suggested this[25].

Some laboratories[26] have found etching to be a viable alternative method for producing tips. Etching in a constant environment tends to produce conical tips. Based on our suggestion, Professor M. Ohtsu, of the Tokyo Institute of Technology, developed a two-step etching process that allows him to change the cone angle along the taper. This double-cone shape might be considered a zeroth order approximation to a positive curvature (or pseudo-parabolic) taper. He found that the tip had dramatically increased throughput[27].

Based on these encouraging results, we propose to develop an etching system with considerably more control. We will continuously vary experimental parameters *during etching* so as to provide a positive curvature *along the entire taper*. While we cannot be sure what the final recipe will entail, it is straightforward to speculate what one might try. For example, the temperature of the etchant can be varied so as to vary the etch rate while slowly pulling the taper from the etching bath. Alternatively, the pH of the etchant can be varied during etching.

We recently began some preliminary etching studies. We studied the role of an etching encapsulant on taper structure and have identified iso-octane as an encapsulant that results in a relatively large (and therefore desirable) apex cone angle of approximately 46°. Our first results also suggest that this angle may be a decreasing function of temperature - as we had expected. We also determined that ultrasonic agitation during etching can results in smoother taper surfaces.

Our goal is to determine a reproducible, controllable method for making tips with a shape and surface well suited for NSOM use. Because the etching process is slow and the paramentes can be easily changed in situ, we are optimistic that we will be successful in combining etching with the pulling technique.

There is an important difference between etched and pulled tips. A pulled tip has an index profile exactly the same, i.e. scaled down in proportion, as the mother fiber. An etched tip on the other hand is all core at

the apex. Its claddding has been etched away. Because of this fundmental difference, we will have to alter our taper optics analysis programs to determine the best shape for a coated etched tip. We will of course do this, and we will correlate predicted performance of etched tips with their measured performance in our attempts to manufacture the most efficient NSOM tip possible.

c. Near-field Modelling Our efforts at modelling the optics of the taper region have proven quite useful. We have determined several taper features that - modelling would suggest - will provide an improved taper. These include a positive curvature along the taper and a fairly large apex angle of approximately 45°. (We call this a "chubby" tip.)

We will extend our assessment of the throughput (T) and the energy sideput into the near-field region. The question of the concentrator efficiency versus its shape is compelling and vital for practical near-field microscopy. We will therefore use both analytical methods (with possible reduction to the scalar field propagation) and numerical modeling, better suited for the input of the actual probe specifications. The axial symmetry of the probe partially simplifies the solution of the multicomponent PDEs (Maxwell's equations). The finite-difference time domain method will be used[28], and the code will be adapted for specific boundary conditions (dielectric interfaces, metal coating). Special care will be taken of the matching the "input boundary" with the results of the far-field analysis. The latter will be based on the fiber mode and/or ray tracing considerations. Our goal will be not the detailed output of the electromagnetic field distribution, but its integral characteristic, energy throughput.   While a number of groups have made important progress in this regard[29, 30], their foci have not been on maximizing probe throughput. However, distorsions of the field, in particular the emerging Z-component will be useful for better understanding of coupling with the Raman-active modes of the sample.

2. **MATERIALS SCIENCE RESEARCH**. As shown in the *Results of Previous Work* section above, we have begun to use NSOM in a variety of exciting materials science investigations. These initial efforts established the broad new capabilities of the NSOM. We now propose to more completely develop two lines of research specifically chosen because of the match between their needs and the capabilities of the NSOM. The chosen materials systems are Mercury Cadmium Telluride and diamond thin films.

a. **Mercury Cadmium Telluride: Materials Issues.** Mercury Cadmium Telluride, $Hg_{1-x}Cd_xTe$ (or MCT), has become a material of choice for IR sensing, especially in the 8-12 μm spectral range. This nonstoicheometric II-IV compound can be presented as an alloy of two binaries, a wide-band-gap CdTe and a the negative band-gap semimetallic HgTe: $Hg_{1-x}Cd_xTe = (HgTe)_{1-x} + (CdTe)_x$. As a result, the band gap can be tuned from -0.3 eV at x=0 to 1.6

12

eV at x=1, with a zero value at x=0.16. The narrow gap and therefore comparable energies of the electronic and phonon excitations make a coupling between the electron and phonon subsystems strong.

Raman spectroscopy provides a useful probe to access the lattice dynamics. It is complicated by the opaque nature of these materials (penetration depth 10-20 nm). Low Raman-scattering efficiencies require high local intensities, which principally can alter the stoichiometry (to degrade, or "fry" the sample). Apart from the unique spatial resolution, NSOM is less invasive technique in the sense that overall heating effect by the probe is much smaller at comparable or even higher local intensities. Indeed, with 1 nW output through 100 nm size aperture, one achieves the level of 10 W/cm^2, quite sufficient for Raman studies in MCT. At the same time, fast cooling of this tiny illuminated spot maintains low level of diffusivity of atoms and reduces the chances of compositional distortions. NSOM, with its spatial resolution, brings new opportunities, as well as new challenges. Several problems associated with HgCdTe synthesis and device fabrication are particularly well suited to NSOM capabilities. Especially, the mapping of strain profiles, defect populations and precipitates with nanometric precision can provide important information not available by other techniques. In the following three paragraphs, we outline several of these problems.

• **Implantation-induced effects.** In many applications, preferred HgCdTe architectures involve extrinsically doped heterostructures[31]. Doping may be undertaken either using grown-in or implantation techniques. The latter enjoys the advantages of being a planar technology that is relatively easy to implement. For p-type doping, arsenic implantation is frequently employed, as for example in the IR-HgCdTe arrays in a joint program at Rockwell and the Night Vision Laboratory. Implantation followed by annealing is an established semiconductor processing technique, but it is not without drawbacks. For HgCdTe heterostructures, for example, compositional redistribution during implantation/annealing differs from what might be classically expected. Compositional redistribution in this system can, however, be controlled in an *ad hoc* manner by varying material structure parameters and implant/anneal conditions. Structural damage and its associated stress is another disadvantage of implantation doping. In practice, activation and annealing drives the dopant ahead of a defective area, and this is where the junction is made.

• **Composition-induced effects.** Compositional variations such as Te precipitation can also be a problem in HgCdTe films themselves as well as in the substrate material. There is a very narrow material growth window of about 5°. On one side of the

13

window one has twinning on the other precipitation. The size of the Te precipitates, as well as possible segregation products for other impurities, lies in the range from 10 nm and higher. In both substrates and the films, micron-sized precipitates can adversely affect the performance of the devices. Associated with the precipitates are strain fields.

• **Interface-induced effects.** Heteroepitaxial films of HgCdTe several microns thick may be grown on CdZnTe, or Si with buffer layers of CdTe or GaAs and CdTe. Interface strain in such structures can induce dislocations in the HgCdTe that can degrade detector performance. The presence of dislocations can be inferred using topographic x-ray techniques, but the depth dependence of the defect distribution and the strain profile is not known.

For all three of these effects, dimensions of interest in the investigation of the problem are in the sub-micron range. NSOM brings to the table its unique capability of providing optical information on such sub-wavelength structures.

b. Mercury Cadmium Telluride: NSOM Studies. We propose to use the NSOM to investigate HgCdTe, and to immediately couple the data into existing and refined material models. Our ability to determine strain profiles and defect densities on the nanometric scale will allow us to provide information that may be used to better study the material synthesis problems outlined above. We will closely relate the experimental data with the modeling of the material, to ensure accurate physical interpretaion and consistency. In particular, we will calculate stress profiles induced by the growth mismatch of precipitates. Lattice dynamics models (only short range forces, no significant Coulomb contribution)[32] will allow us to estimate the expected changes in the phonon frequencies and their manifestation in the Raman spectra.

HgCdTe is Raman-active, and a number of studies have employed this property in investigations of material properties. The effect may be used to study lattice dynamics and electronic behavior[33-35], quantum confinement[36], structural ordering[37], and alloy composition and crystallinity[38]. The phonon frequencies observed in such Raman studies are affected by strain. In fact, most qualitative features of the compositional dependence of the observed optical phonons can be explained - at least partially - in terms of strain effects[39].

Conventional HgCdTe Raman studies must be undertaken at cryogenic temperatures[35]. As we mentioned above, nano-Raman studies may not

14

require refrigeration. It is difficult to predict *a priori* with certainty if cryogenic techniques must be employed. If this turns out to be the case, however, we have experience to draw on. Several years ago, we were the first laboratory to demonstrate that NSOM investigations could be carried out at liquid nitrogen temperatures[5]. While we have not yet undertaken Raman measurements below room temperature, our Raman microscope was built to fit into a dewar, and we anticipate no fundamental problems in extending Raman studies to the lower temperatures.

In the Rockwell/Night Vision study, implanted 40μmx40μm arrays are doped by implantation. Of interest are the strain profile and the defect density around the implanted region. NSOM Raman imaging would deepen our understanding of the annealing-related strain relief. Time-resolved NSOM studies would provide information about the evolution of defect profiles during the annealing process. We will also perform mathematical modeling of chemical diffusion of the dopant and the host-components, in attempts to explain observed anomalies. Possible enhancement of the diffusion by the dopant via a kick-out mechanism[40] and stress-induced diffusion[41, 42] must be taken into consideration. All of this information would lead to better control of the entire doping procedure.

Precipitate morphologies and distributions could likewise be studied with nanometric precision using NSOM. The micron-sized Te precipitates are too small to study using conventional microscopic techniques but are well above the resolution limit for current NSOM technologies. The added knowledge provided by the NSOM could lead to better control of precipitates and improved substrate and device fabrication.

Dislocations and strains associated with heterostructures can also be investigated with the NSOM. In this case, cleaving of an epi-layer to reveal the interface in cross section would be necessary. Although somewhat more difficult to work with than a planar sample, such structures have been imaged in an NSOM. All that is required is a 2 μm square region that is relatively flat. Such a surface is routinely obtained when cleaving HgCdTe heterostructures. As suggested above, more information on the nanometric scale about sample morphology, defect populations, and strain profiles would lead to a deeper knowledge and better control of material quality.

For all of the Raman studies, lateral resolution would be determined by the near-field probe employed. Axial resolution - i.e. depth resolution into the sample - is determined by the penetration depth of the incident radiation used in nano-Raman near-field studies. In a series of conventional micro-Raman studies[17, 18] we have shown that it is possible to fold out the depth profile of stress by analyzing stress-induced shifts in Raman features for a variety of laser lines and thus a variety of penetration depths. The axial resolution obtained in such studies can be on the order of ten nanometers,

even for conventional optical systems. Direct application of such a technique to near-field investigations is complicated by the fact that the optical field profile diverges rapidly with distance from the near-field probe apex. Nonetheless, some determination of the depth dependence of the would certainly be possible. Once we have determined lateral profiles across sample surfaces, we will measure the depth dependence of the stress in this manner.

Our ability to view defect populations by employing time-resolved imaging techniques is likewise well-suited to the study of HgCdTe. Our initial studies of Si defects[13, 21, 22] can easily be extended to HgCdTe. Some adaptation of the experimental set-up will be required because of the narrow band gap of the HgCdTe. We have in our laboratory, however, a HeNe laser fitted with mirrors to allow us to use 3 μm radiation for the infrared probe radiation. Free carriers can be excited with any of a number of available laser lines.

NSOM mapping of defects in the vicinity of implantation-induced, composition-induced, and interface-induced effects will allow us to study the generation and dynamics of the effects with sub-wavelength precision. Of particular value will be the coupling of defect mapping with the stress profiles obtained through nano-Raman investigations. In our theory-modeling effort we envisage a coordinated effort on three levels:

- Macroscopic, continuum elasticity theory will allow us to estimate the stress fields originating usually from the mismatch in epitaxial growth, and from the incommensurate precipitates if such form.

- Stress values can be fed into the standard lattice-dynamics models to calculate the expected changes in the Raman spectra.

- In a kinetic analysis, we will attempt to calculate stress-induced diffusion, which has to be added into the standard chemical difffusion equations in order to explain measured profiles of both implanted (e.g. As) and host (Hg and Cd) components.

MCT samples to be investigated will be obtained in a collaborative effort with colleagues at the Night Vision Laboratory[43] who co-ordinate materials synthesis and processing programs at Rockwell and Highes (SBRC) with analysis efforts. Our NSOM studies will thus be added to the usual analytical methods used to advance MCT science and technology.

c. **Diamond Films: Materials Issues.** Diamond's physical properties make it a material of interest in a wide range of application[44]. Its high thermal conductivity and low electrical conductivity suggest applications in thermal management for high-speed electrical circuits, laser-diodes used in

16

communication, and fast computers. With a band-gap well into the ultraviolet, diamond has been touted as a semiconductor that could be used high temperature high voltage applications. Similarly diamond LEDs or lasers could operate in the UV.

Production of semiconductor grade diamond of macroscopic dimensions remains illusive. A number of techniques have been employed in attempts to produce such material. These include, for example, plasma enhanced CVD, hot wire CVD, reactive vapor deposition, ion beam asisted deposition, and laser CVD. Plasma enhanced CVD deposition has resulted in large polycrystalline wafers as large as 150 mm in diameter and 0.5 mm thick. Even for such a method, however, deposition rates are still painfully slow and the efficiency of carbon incorporation far too small to consider commercialization.

Progress in diamond thin film syntheses has involved study of the deposition process and systematic control of deposition parameters. What is needed is a deeper *fundamental* understanding of diamond thin film synthesis.

A satisfying full model of crystal growth has not been developed for diamond films. While electron micrographs indicate crystallite morphology and orientation, modelling of the growth of the diamond film requires an understanding of the nucleation and crystallization processes. In order to understand the growth mechanism of diamond crystals, information regarding the evolution of surface morphology and its dependence on deposition conditions is needed. A correlation of bonding configuration and local strain with crystallite morphology would help considerably in uncovering the dynamics of nucleation and growth. This, in turn, could lead to synthesis of higher quality films at faster deposition rates.

d. Diamond Films: NSOM Studies. We propose to use the NSOM to investigate thin diamond films. Our ability to determine strain profiles and bonding statistics on the nanometric scale will allow us to provide information that may be used to better study materials synthesis. We already have experience examining diamond films using conventional Raman spectroscopy[45]. We now will extend our efforts to add nanometric imaging to the analysis.

The Raman active mode of diamond has T_{2g} symmetry. The first order band of this feature indicative of sp^3 bonding occurs at 1332 cm^{-1}. In our earlier work on diamond shown in figure 7, we compared the 8 cm^{-1} width of this line to the theoretical single crystal width of 2 cm^{-1}. The broad weaker band at 1580 cm^{-1} is indicative of sp^2 bonds. Although not examined in the work shown in the figure, the position of the 1332 cm^{-1} peak can be used to measure stress in the material.

17

Figure 7.

MicroRaman spectra of CVD diamond films. The band at 1332 cm^{-1} indicates a presence of crystalline-like sp^3 bonding. The broad band at $1580cm^{-1}$ indicates the presence of graphitic sp^2 bonding[45].
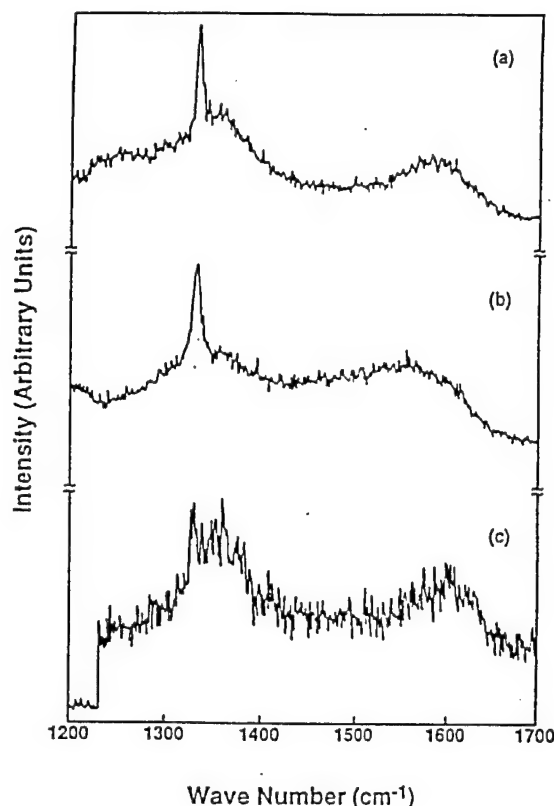
While the data shown here are of some interest, much more valuable would be similar data taken with an NSOM. As we have shown in our studies of KTP, Raman spectra taken over regions of nanometric dimensions can be obtained in an NSOM. In such NSOM images and spectra, the local bonding and stress around the diamond nuclei could be measured. As taper development succeeds in providing us with higher efficiency tips, NSOM images taken within the 1332 cm^{-1} line would provide us with a revealing bonding map of the diamond films.

Defect population images would also aid in understanding of nucleation and growth processes in diamond film synthesis. There is no fundamental reason why our defect imaging studies (that have proven so successful on silicon) could not be extended to include investigation of the wide-band-gap semiconductor that diamond is. Of course, the spectral range of the experiment would have to be extended to the ultraviolet. With frequency-doubling capabilities that we have in-house, operation in the uv is possible. If it is possible to measure free-carrier absorption due to uv photo-excited carriers, defect imaging may be possible. We will pursue this avenue if initial studies are promising.

18

Diamond samples to be investigated will be obtained from researchers on our campus[46] who employ CVD methods to obtain polycrystalline samples. The samples obtained are quite planar. This is an important consideration in NSOM applications where highly corrugated samples are difficult to image because of the difficulty in interpreting optical signals when tip vertical excursions are roughly the same size as the tip aperture.

5. LIST OF PUBLICATIONS AND TECHNICAL REPORTS

Prior to 1995 on previous ARO-supported research, 12 other articles appeared in refereed journals. For the specific work undertaken during the duration of the grant reprted on here, the following publications appeared.

1. "Tip Optics for illumination NSOM: extended-zone approach," B.I. Yakobson and M.A. Paesler, Ultramicrsocopy, 57, 204 (1995).

2. "Kinetics, morphology, and pulling regimes for sensing tips in near-field microscopy," B.I. Yakobson and M.A. Paesler, Ultramicroscopy, 57, 241 (1995).

3. "The Huygens-Fresnel Principle in the near-field," F. Depasse, M.A. Paesler, D. Courjon, and J.M. Vigoreuz, Optics Letters 20, 234 (1995).

4. "Thermal/Temporal Response of the NSOM Probe/Sample System," H.D. Hallen, B.I. Yakobson, A. LaRosa, and M.A. Paesler, SPIE 2535, 34 (1995).

5. "Nano-Raman spectroscopy and imaging with near-field scanning optical microscope," chapter in *Raman Microscopy and Imaging*, A.B. Myers, ed. John Wiley & Sons, New York, 1996.

6. "Near-field Optics," Symposium Proceedings of the International Society for Optical Engineering, M.A. Paesler, and P.J. Moyer, editors, SPIE, Bellingham, WA, 1995.

7. "Proceedings of the 3rd Int. Conf. on Near-field Optics," M.A. Paesler and N.F. VanHulst, editors, Elsevier, Amsterdam, 1995.

8. "Thermal/Optical Effects in NSOM Probes," B.I. Yakobson, A. LaRosa, H.D. Hallen, and M.A. Paesler, Ultramicroscopy, 61, 179, (1995).

9. "Raman imaging with near-field scanning optical microscopy," C.L. Jahncke, M.A. Paesler, and H.D. Hallen, Appl. Phys. Lett. 67, 2483 (1995).

10. "Time-resolved contrast in near-field scanning optical microscopy of semiconductors," A.H. LaRosa, C.L. Jahncke, and H.D. Hallen, SPIE **2384**, 101 (1995).

11. *Near-field Optics: Theory, Practice, and Applications*, M.A. Paesler and P.J. Moyer, John Wiley & Sons, New York, 1996.

12. "Origins and effects of thermal process on near-field optical probes," A.H. LaRosa, B.I. Yakobson, and H.D> Hallen, Appl. Phys. Lett. **67**, 2597 (1995).

13. "Energy Dissipation in NSOM Probe Fiber Tapers: Ray Tracing Assessment," P. O. Boykin, M. A. Paesler, B. I. Yakobson, Biomedical Fiber Optics, Abraham Katzir and Jay Harrington, eds. SPIE <u>2677</u>, 148-153 (1996).

14. "Near-field Optical Spectroscopy: Enhancing the Light Budget," M.A. Paesler, H.D. Hallen, B.I. Yakobson, C.J. Jahncke, P.O. Boykin, and A. Meixner, Microscopy and Microanalysis **3**, 815 (1997).

15. "Optical imaging of carrier dynamics in silicon with subwavelength resolution," A.H. LaRosa, B.I. Yakobson, and H.D. Hallen, Appl. Phys. Lett. **70**, 1656 (1997).

6. LIST OF PARTICIPATING PERSONNEL

Faculty
- PI   Michael Paesler, Professor
- co-PI   Boris Yakobson, Associate Research Professor

Former Students
- Patrick Moyer, PhD 1993
  Assistant Professor, Physics Dept., UNC-Charlotte
- Catherine Jahncke, PhD 1994
  Assistant Professor, Physics Dept., St. Lawrence University
- Andres LaRosa, PhD 1995
  Firmenich Inc., Princeton, NJ
  Applied Research Dept., - Physical Measurements

Present Students
- Suzanne Huerth
- Stephen Winder

The US Army Research Office has provided important seminal support for efforts in near-field optics. The academic program at NC State has been particularly successful, producing three PhDs and a significant body of original research. All three PhD students who obtained their degrees are maintaining their interests in near-field optics. Two (Patrick Moyer and Catherine Jahncke) are assistant professors in tenure-track positions with ongoing research in the field. The third (Andres LaRosa) is employed in an industrial optics applied research laboratory.

In keeping with the ARO goal of supporting research that leads to rapid technology transfer, it should be mentioned that before entering the academic world, Dr. Moyer developed the first commercial NSOM for *Topometrix*. Within 6 months of obtaining his ARO-supported degree, he had brought the technology to the marketplace. To date, the instrument he developed is still the only commercially available NSOM. There are approximately 100 instruments in use today. Many of the innovations developed in our laboratory have been incorporated into the *Topometrix* instrument. Our proposed work will also no doubt lead to technological advances that will ultimately make it to the marketplace.

7. BIBLIOGRAPHY

1. E. Betzig, J.K. Trautman, T.D. Harris, J.S. Weiner, and R.L. Kostelak, Science **251**, 1468 (1991).

2. D.W. Pohl, in *Advances in Optical and Electron Microscopy*, edited by C.J.R. Sheppard and T. Mulvey (Academic, London, 1990), pp. 243-312.

3. J.K. Trautman, E. Betzioog, J.S. Weiner, D.J. DiGiovanni, T.D. Harris, F. Hellman, and E.M. Gyorgy, J. Appl. Phys. **71**, 4659 (1992).

4. A very complete, but as yet somewhat inaccessible compendium of current research in near-field optics appears as: Proceedings of the *First Interantional Conference on Near Field Optics*, Besançon, 1992, in press.

5. A. Korpel, in reference 4.

6. C.W. McCutcheon, Rev. Sci. Instrum. **35**, 1340 (1964).

7. J.M. Guerra, Applied Optics **29**, 3741 (1990).

8. E.L. Buckland, P.J. Moyer, and M.A. Paesler, J. Appl. Phys. **73**, 1018 (1992); and in reference 4.

9. B.I. Yakobson, P.J. Moyer and M.A. Paesler, J. Appl. Phys. **73**, 7984 (1993).

10. R. Ruppin, Surface Science **127**, 108 (1983).

11. E. Betzig, A. Harootunian, M. Isaacson, and E. Kratschmer, Biophys. J. **49**, 269 (1986).

12. E. Marx, and E.C. Teague, Appl. Phys. Lett. **51**, 2073 (1987).

13. M.A. Paesler, P.J. Moyer, and C.J. Jahncke, Phys. Rev. B **42**, 6750 (1990).

14. P.J. Moyer and M.A. Paesler, J. Appl. Phys, in press.

15. P.J. Moyer and M.A. Paesler, in reference 4.

16. D.J. Thiel, D.H. Bilderback, A. Lewis, E.A. Stern, and T. Rich, Applied Optics, **31**, 987 (1992).

17. W.T. Vetterling, and R.V. Pound, J. Opt. Soc. Am., **66**, 1048 (1976).

18. R. Collins and M.A. Paesler, Solid State Commun. **34**, 833 (1980).

19. Y. Kirino, and F. Shimura, J. Appl. Phys **69**, 2700 (1991).

20. D.L. Polla, IEEE Electron. Dev. Lett., EDL-**4**, 185 (1983).

21. M.A. Tamar, ed., Diamond-Film Semiconductors, SPIE v. 2151, 1995.

22. "Porous Silicon and Related Materials," European Materials Research Society Proceedings, vol. 51, 1996.

23. R.G. Sparks and M.A. Paesler, J. Appl. Phys., **71**, 891 (1992).

24. Mann, J.V. Bannister, and R.J.P. Williams, J. Mol. Bio. **188**, 225 (1986).